

Wave propagation in nonlinear left-handed transmission line media

Alexander B. Kozyrev,^{a)} Hongjoon Kim, Abdolreza Karbassi, and Daniel W. van der Weide
Department of Electrical and Computer Engineering, University of Wisconsin—Madison, Madison, Wisconsin 53706

(Received 29 April 2005; accepted 27 July 2005; published online 14 September 2005)

Using a one-dimensional system, we demonstrate a wide variety of wave propagation phenomena possible in nonlinear left-handed media. These include effective second-harmonic generation where the fundamental wave and the second-harmonic wave are badly mismatched. We also observe parametric instabilities accompanying intensive harmonic generation. © 2005 American Institute of Physics. [DOI: 10.1063/1.2056581]

Negative-refractive-index metamaterials, also known as left-handed (LH) media, first postulated by Veselago,¹ are now being demonstrated in resonant rf and microwave circuits.^{2–5} The majority of studies and applications of one- and two-dimensional LH media to date are in the linear regime of wave propagation.⁶ However, materials that combine nonlinearity with anomalous dispersion exhibited by LH media have also recently attracted much attention. Nonlinear properties of left-handed metamaterials, as well as some approaches to make metamaterials nonlinear, have been discussed in several publications.^{5,7–17} We have presented a theoretical investigation of the basic nonlinear wave propagation phenomena in LH medium,¹⁷ which is based on the dual of the conventional nonlinear transmission line (NLTL), a left-handed (LH) NLTL exhibiting anomalous dispersion. The transmission line approach we used proved to be a realistic description of the LH media. It provides insight into the physical phenomena of LH media and is an efficient design tool for LH applications.⁴ We found that nonlinear wave form evolution in a LH NLTL can be understood in terms of competition between harmonic generation and parametric instabilities.

Confirming our general predictions,¹⁷ we present here the first experimental results for harmonic generation and parametric generation in 1D left-handed NLTL media operating in the microwave regime. Understanding of the nonlinear phenomena in LH NLTL media is very important for both the development of new types of devices and improvement of the performance of recent tunable devices based on LH NLTLs like phase shifters,⁵ tunable leaky-wave antennas^{4,18} and notch filters.¹⁶

We fabricated one-dimensional nonlinear LH media, four- and six-section LH NLTLs having identical sections [Fig. 1(a) shows a 4-section LH NLTL]. Circuits were realized on Rogers RT/Druid 3010 board with $\epsilon_r=10.2$ and thickness $h=1.27$ mm. A row of $0.5\text{ mm}\times 0.5\text{ mm}$ copper pads separated by 0.2 mm gaps was formed on the surface of the Rogers board by standard lithography. M/A-COM hyper-abrupt junction GaAs flip-chip varactor diodes (MA46H120) were attached between these pads using conductive silver epoxy. The C_{j0} of the diodes, from the manufacturer's data sheet, is 1.1 pF , and they show a capacitance ratio $C(0\text{ V})/C(10\text{ V})=7.5$. The nonlinear capacitance in each section is formed by two back-to-back diodes with dc bias

applied between them. Shunt inductances were implemented with 0.12-mm-diam copper wires connecting the pads to the ground plane on the back side of the board. The via holes were drilled 1.8 mm from the pads so that the total length of these inductance wires was 3.2 mm . Direct current bias wires were connected with $3\text{ k}\Omega$ resistors between diodes as shown in Fig. 1(b). The pads on the board surface, together with inherent parasitics, introduce unavoidable series inductance and shunt capacitance, making the whole circuit a composite right/left-handed transmission line having the equivalent circuit shown in Fig. 1(b). Figure 2 shows the magnitude and phase of the linear wave transmission (S_{21}) of the LH NLTLs. The high-pass Bragg cutoff frequency, and the dependence of phase on frequency, indicate the left-handed nature of the system. We measured a -6 dB cutoff frequency at 2.7 GHz for 0 V bias. The left-handed passband corresponds to a variation of the total phase delay of 4π in the four-section LH NLTL case and 6π in the six-section LH NLTL case. The frequency region from 2.7 to 8 GHz for 0 V bias corresponds to the left-handed passband. Parameters of the circuit model in Fig. 1(b) were extracted from the S parameters measured at 0 V bias. They are $C_L=0.99\text{ pF}$, $L_L=1.695\text{ nH}$, $C_R=0.05\text{ pF}$, $L_R=0.966\text{ nH}$.

Nonlinear wave form evolution in LH NLTLs is qualitatively different from wave form evolution in conventional right-handed (RH) NLTLs. Propagation of a large-amplitude sinusoid in RH NLTLs results in edge steepening, leading to shock wave formation; the spectrum of the wave form at the output contains the fundamental together with its higher harmonics, whose amplitudes decay with frequency.^{19,20} Effective harmonic generation is enabled by phase matching the

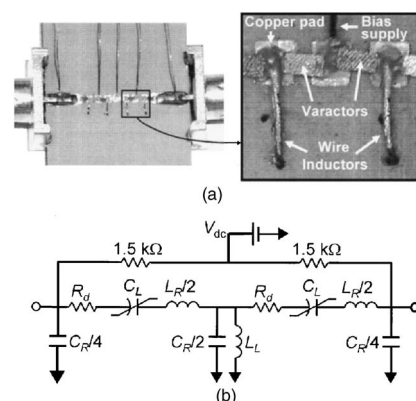


FIG. 1. (a) Fabricated LH NLTL and (b) equivalent circuit of one stage.

^{a)} Author to whom correspondence should be addressed; electronic mail: abkozyrev@wisc.edu

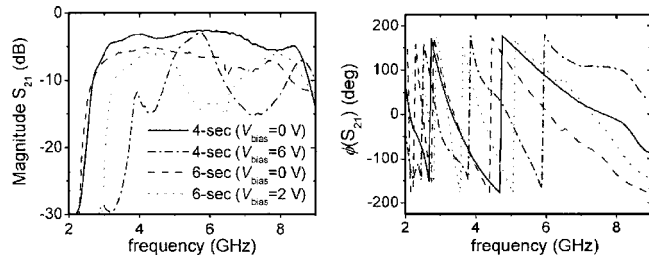


FIG. 2. Measured magnitude and phase of S_{21} parameter for four- and six-section LH NLTLs.

fundamental with its higher harmonics. The impossibility of shock wave formation in LH NLTL enables complicated nonlinear phenomena from the interplay of higher harmonic generation and parametric instabilities due to interaction of counter-propagating waves enabled by anomalous dispersion.

Both simulation¹⁷ and our experiments with LH NLTLs confirm that harmonic generation dominates over parametric instabilities in short LH NLTLs. The amplitude of the second harmonic in the n th section of a LH NLTL $V_2(n)$ can be obtained using a small signal approach described in Ref. 17

$$|V_2(n)| \approx \frac{4K_N V_1^2(0) \sin^2\left(\frac{\beta_1}{2}\right) \cdot \sin^2(\beta_1)}{\sin\left(\frac{\beta_2}{2}\right) \cdot \left[\sin^2\left(\frac{\beta_2}{2}\right) - \sin^2(\beta_1) \right]} \cdot e^{-\alpha n} \cdot |\sin[(\beta_2 - 2\beta_1)n/2]|, \quad (1)$$

where K_N is a “nonlinearity factor” dependent only on diode parameters, $V_1(0)$ is the voltage at the input of the LH NLTL, α is the attenuation constant, n is the section number and β_1 and β_2 are propagation constants (phase shift per section) for the fundamental wave and its second harmonic, respectively.

The fundamental wave propagating in the LH NLTL is always badly mismatched with its higher harmonics due to inherent anomalous dispersion, yet the generation of higher harmonics can still be very effective. This is possible because of “amplitude singularities.” The denominator in Eq. (1) has zeros when

$$\sin^2(\beta_2/2) - \sin^2(\beta_1) \rightarrow 0. \quad (2)$$

For example, using circuit parameters extracted from measured S parameters, this occurs when $\beta_1=2.776$ and $\beta_2=0.731$. Due to phase mismatch, the amplitude of the second harmonic varies rapidly with distance. This gives rise to a highly localized energy exchange between the fundamental wave and its second harmonic. It is apparent from Eq. (1) that the maximum amplitude of the second harmonic at the end of the N -section line is achieved when

$$(\beta_2 - 2\beta_1)N = (2k + 1)\pi, \quad k = 0, 1, 2, 3, \dots \quad (3)$$

The same approach applied to RH NLTL predicts linear growth of the second-harmonic amplitude (in lossless case) due to its phase matching with fundamental wave.^{17,21} Thus, the theoretical analysis of second-harmonic generation in LH NLTLs shows that, despite the large phase mismatch, inherent anomalous dispersion enables the possibility of faster-than-linear growth of the second-harmonic amplitude as predicted by Eq. (1) in a narrow frequency range where condition (2) is satisfied. A somewhat similar singular behavior

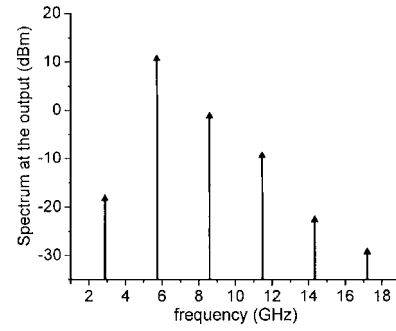


FIG. 3. Spectrum of the output wave form generated by a four-section LH NLTL fed by 2.875 GHz, +17.9 dBm input signal at reverse bias voltage of 6.4 V.

of the second-harmonic amplitude was predicted for the wave reflected from a slab of nonlinear LH medium.¹⁴

The measured results qualitatively confirm our predictions using small-signal analysis. Figure 3 shows the spectrum of the wave form from the output of four-section LH NLTL as measured with an Agilent E4448A Spectrum Analyzer, and corresponds to the maximum of the second-harmonic conversion efficiency. The measured value for the second-harmonic conversion efficiency in this four-section LH NLTL was 19% using a 2.875 GHz, +17.9 dBm input signal and a reverse bias voltage of 6.4 V. The second-harmonic power delivered into a 50Ω load was +10.72 dBm. The fundamental wave is close to the Bragg cutoff frequency [note the magnitude of S_{21} for the four-section LH NLTL at bias voltage 6 V as shown in Fig. 2(a)], and thus falls into frequency range for which small signal analysis predicts amplitude singularity. The second-harmonic wave is close to the transmission maximum, which is located in the middle of the left-handed passband. A fundamental of 2.875 GHz generates numerous higher harmonics, with the second harmonic dominating over the fundamental and the other harmonics. Thus, the LH NLTL combines the properties of both a harmonic generator and a bandpass filter, and under certain conditions may provide an almost pure higher harmonic at its output.

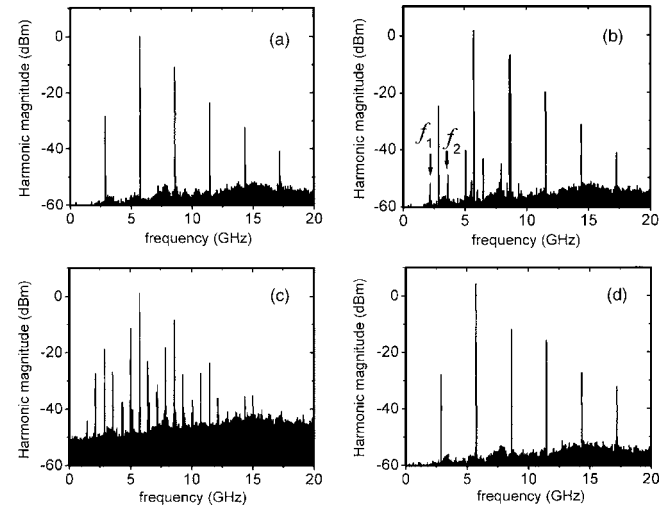


FIG. 4. Spectra of the output wave form generated by a four-section LH NLTL fed by 2.875 GHz, +19 dBm input signal for different values of the bias voltage (a–4 V, b–4.95 V, c–5 V, d–6.3 V). The results here are decreased by 6 dB due to a protection attenuator.

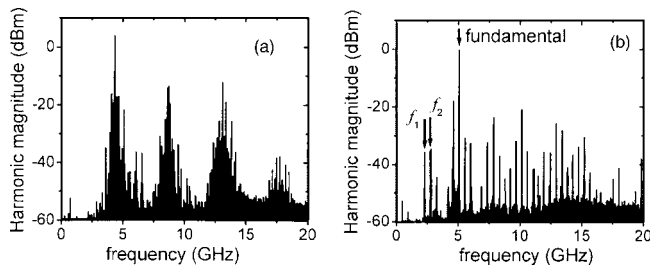


FIG. 5. Spectra of the output wave form generated by six-section LH NLTL fed by (a) 4.34 GHz, +29 dBm input signal and (b) 5.074 GHz, +29 dBm input signal at reverse bias voltage of 6.9 V. The results here are decreased by 6 dB due to a protection attenuator.

The conversion efficiency observed in the LH NLTL is comparable with the per-stage efficiency of a hybrid Schottky-diode RH NLTL operated in a lower frequency range.²²

Under certain circumstances, harmonic generation may compete with different parametric processes, resulting in unstable harmonic generation.¹⁷ The anomalous dispersion of LH NLTLs enables effective basic parametric interactions of the type

$$f_1 + f_2 = f_3, \quad \beta_1 - \beta_2 = \beta_3, \quad (4)$$

where the high-frequency pump wave with frequency f_3 and wave number β_3 generates two other waves. The wave with frequency f_2 propagates in the opposite direction relative to the pump wave and the wave having frequency f_1 . From a previous analysis,⁷ for the lossless case, the frequencies and powers of these waves also obey the nonlinear Manly–Rowe relations.

A wave at 2.875 GHz cannot parametrically generate any other waves since they would exist below the line's cut-off frequency. However, an intensive second-harmonic wave may initiate the parametric process. The second harmonic at 5.75 GHz excites waves with frequencies of 2.2 and 3.55 GHz depicted in Fig. 4(b) as f_1 and f_2 . This basic parametric process then initiates multiple higher-order parametric interactions, resulting in multiple peaks in the spectrum of the output wave form. The progression of this process is shown in Fig. 4(c), which illustrates conversion of a monochromatic input signal into a wideband output. Further increase of the reverse bias voltage leads to the stabilization of the harmonic generation and suppression of parametric instability [Fig. 4(d)].

Although higher harmonic generation dominates in short LH NLTLs, in longer transmission lines parametric interactions predominate. Figure 5 shows spectra at the output of a six-section LH NLTL. At some input signal and reverse bias voltage values, the peaks corresponding to the fundamental wave and the higher harmonics become broad, thus restricting the peak second-harmonic conversion efficiency. Figure 5(b) demonstrates conversion of a 5.074 GHz, +29 dBm input into a wideband output initiated by basic parametric process involving a fundamental pump wave of 5.074 GHz and two other waves having frequencies of 2.274 and 2.8 GHz [depicted in Fig. 5(b) as f_1 and f_2].

Our measurements demonstrate efficient higher-harmonic generation using LH NLTLs. Harmonic generation is possible at higher frequencies in comparison with the conventional dual low-pass filter NLTLs. Furthermore, LH NLTLs are predicted to have advantages from the design perspective, since we have more freedom to optimize parameters, being much less restricted by the host waveguide structure than in the case of RH periodically loaded NLTLs. They are more compact since the length of the section in practice is determined by the diode. Furthermore, extending these results for one-dimensional LH NLTLs to higher dimensions would enable combining harmonic generation in LH NLTL media with focusing, due to the negative refractive index of two- or three-dimensional LH transmission line media. This may lead to the development of highly efficient and powerful frequency multipliers. Moreover, our approach could be scaled from its current X-band form into THz, infrared, or ultimately visible form.²³ The parametric generation and amplification that generally accompany harmonic generation in LH NLTLs will be of interest for building “active” or “amplifying” super lenses based on LH nonlinear medium and provide a means to compensate for the inherent LH medium loss which is a current challenge for existing LH materials.

This work has been supported by AFOSR through the MURI program under Grant No. F49620-03-1-0420.

- ¹V. G. Veselago, *Sov. Phys. Usp.* **10**, 509 (1968).
- ²R. A. Shelby, D. R. Smith, and S. Schultz, *Science* **292**, 77 (2001).
- ³G. V. Eleftheriades, A. K. Iyer, and P. C. Kremer, *IEEE Trans. Microwave Theory Tech.* **50**, 2702 (2002).
- ⁴A. Lai, C. Caloz, and T. Itoh, *IEEE Microw. Mag.* **5**, 34 (2004).
- ⁵H. Kim, A. B. Kozyrev, and D. W. van der Weide, *IEEE Microw. Wirel. Compon. Lett.* **15**, 366 (2005).
- ⁶K. Y. Bliokh and Y. P. Bliokh, *Physics-Uspexhi* **47**, 393 (2004).
- ⁷A. S. Gorshkov, G. A. Lyakhov, K. I. Voliak, and L. A. Yarovoii, *Physica D* **122**, 161 (1998).
- ⁸A. M. Belyantsev and A. B. Kozyrev, *Tech. Phys.* **46**, 864 (2001).
- ⁹A. M. Belyantsev and A. B. Kozyrev, *Tech. Phys.* **47**, 1477 (2002).
- ¹⁰A. A. Zharov, I. V. Shadrivov, and Y. S. Kivshar, *Phys. Rev. Lett.* **91**, 037401 (2003).
- ¹¹M. Lapine, M. Gorkunov, and K. H. Ringhofer, *Phys. Rev. E* **67**, 065601 (2003).
- ¹²M. Lapine and M. Gorkunov, *Phys. Rev. E* **70**, 066601 (2004).
- ¹³C. Caloz, I. H. Lin, and T. Itoh, *Microwave Opt. Technol. Lett.* **40**, 471 (2004).
- ¹⁴V. M. Agranovich, Y. R. Shen, R. H. Baughman, and A. A. Zakhidov, *Phys. Rev. B* **69**, 165112 (2004).
- ¹⁵I. V. Shadrivov, A. A. Sukhorukov, Y. S. Kivshar, A. A. Zharov, A. D. Boardman, and P. Egan, *Phys. Rev. E* **69**, 016617 (2004).
- ¹⁶I. Gil, J. Garcia-Garcia, J. Bonache, F. Martin, M. Sorolla, and R. Marques, *Electron. Lett.* **40**, 1347 (2004).
- ¹⁷A. B. Kozyrev and D. W. van der Weide, *IEEE Trans. Microwave Theory Tech.* **53**, 238 (2005).
- ¹⁸D. F. Sievenpiper, *IEEE Trans. Antennas Propag.* **53**, 236 (2005).
- ¹⁹A. V. Gaponov, L. A. Ostrovskii, and G. I. Freidman, *Radiophys. Quantum Electron.* **10**, 772 (1967).
- ²⁰D. W. van der Weide, *Appl. Phys. Lett.* **65**, 881 (1994).
- ²¹K. S. Champlin and D. R. Singh, *IEEE Trans. Microwave Theory Tech.* **MTT-34**, 351 (1986).
- ²²J.-M. Duchamp, P. Ferrari, M. Fernandez, A. Jrad, X. Melique, J. Tao, S. Arscott, D. Lippens, and R. G. Harrison, *IEEE Trans. Microwave Theory Tech.* **51**, 1105 (2003).
- ²³G. Goussetis, A. P. Feresidis, S. Wang, Y. Guo, and J. C. Vardaxoglou, *J. Opt. A, Pure Appl. Opt.* **7**, S44 (2005).